Fabrication of perovskite-type Ba(Sn$_{1-x}$Ta$_x$)O$_3$ ceramics and their power factors

Masao Takada · Hideki Taguchi · Masaki Kato · Ken Hirota

Abstract Perovskite-type Ba(Sn$_{1-x}$Ta$_x$)O$_3$ (0.01 ≤ x ≤ 0.06) ceramics with high relative densities (92.7–94.4 %) were fabricated using the hot isostatic pressing (HIP) method at 1273 K and 196 MPa for 4 h in an atmosphere of argon gas. The lattice parameter decreased slightly with increasing x. From the XPS measurement, the Ta^{5+} ion was stable in Ba(Sn$_{1-x}$Ta$_x$)O$_3$ ceramics and the broad peak of the Ta4f level was the overlap between the Ta^{5+}4f$_{5/2}$ and Ta^{5+}4f$_{7/2}$ levels. Ba(Sn$_{1-x}$Ta$_x$)O$_3$ ceramics were n-type semiconductors, and their electrical resistivities increased with increasing x. The increase in the electrical resistivity was explained by impurity scattering due to the presence of the Ta ions. The absolute value of the Seebeck coefficient (S) increased with increasing temperature and x. The power factor (S^{2}σ), which was calculated from electrical conductivity (σ) and the Seebeck coefficient, was ca. 1.0 × 10^{-5} W m^{-1} K^{-2} at x = 0.01.

Introduction

BaSnO$_3$ has a cubic perovskite-type structure with a = 4.116 Å and behaves as an n-type semiconductor with a band gap of 3.4 eV [1, 2]. The Seebeck coefficient (S) of

M. Takada · M. Kato · K. Hirota
Department of Molecular Chemistry and Biochemistry, Faculty of Science and Engineering, Doshisha University, Kyo-Tanbe 610-0321, Japan

H. Taguchi (✉)
The Graduate School of Natural Science and Technology (Science), Okayama University, 3-1-1 Tsushima-Naka, Kita-Ku, Okayama 700-8530, Japan
e-mail: htaguchi@cc.okayama-u.ac.jp

BaSnO$_3$ was reported to be ca. −300 µV/K at 900 K [3]. Upadhyay et al. measured the electrical conductivity (σ) of BaSnO$_3$ from 310 to 520 K at 0, 1, 10, and 100 kHz [4]. The dc electrical resistivity (ρ$_{dc}$) is 1.6 × 10^9 Ω cm or more below 350 K and decreases linearly with the rise of temperature. Since the sample was prepared at very high temperature, a slight amount of oxygen was lost from the sample. Since the released electrons were caught by the Sn^{4+} ion to generate the Sn^{2+} ion, electrical conduction was explained by the hopping of charge carriers between the Sn^{4+} and Sn^{2+} ions. According to Trari et al. [5] (Ba$_{1-x}$La$_x$)SnO$_3$ (0 ≤ x ≤ 0.02), which was synthesized using a solid-state reaction, is metallic at least for x ≥ 0.0025. Its electrical resistivity is independent of temperature and varies strongly with increasing x. The absolute value of the Seebeck coefficient increases with the rise of temperature and exhibits a large value (ca. −120 µV/K for x = 0.001) at 300 K.

Yasukawa et al. synthesized Ba(Sn$_{1-x}$Co$_x$)O$_3$ using a solid-state reaction and measured both electrical conductivity and the Seebeck coefficient [6]. The samples have a relative density of ca. 95 % and are p-type semiconductors. Electrical conductivity is 10^{-1}–10^2 Ω^{-1} m^{-1} in the measured temperature range and increases with increasing x. They proposed that p-type conduction occurs by the hopping of holes between the localized states of the Co ions. The Seebeck coefficient increases with the rise of temperature and exhibits a large value (ca. 80 µV/K) at 770 K. The power factor (S^{2}σ) is frequently used to evaluate the performance of thermoelectric materials. The sample (x = 0.15) has a high power factor (ca. 2.7 × 10^{-7} W m^{-1} K^{-2}) at 1073 K.

According to Singh et al. [7], the electrical resistivities of the Ba(Sn$_{1-x}$Nb$_x$)O$_3$ ceramics that were sintered at high temperatures decreases with increasing x, has a minimum

value at $x = 0.01$, and then increases with increasing x. The decrease in the electrical resistivity in the range of $0.001 \leq x \leq 0.01$ was explained by the electrons released from both the Nb ion and an oxygen vacancy. On the other hand, the increase in the electrical resistivity in the range of $0.01 \leq x \leq 0.10$ was explained by impurity scattering due to the presence of the Nb^{5+} ions. To improve the power factor of $BaSnO_3$, electrical conductivity must be increased. In the present study, $Ba(Sn_{1-x}Ta_x)O_3$ ceramics with high relative densities were fabricated using the hot isostatic pressing (HIP) method. Electrical conductivity and the Seebeck coefficient were measured to investigate the potential of these oxides as thermoelectric materials.

Experimental

The $Ba(Sn_{1-x}Ta_x)O_3$ samples were prepared by a solid-state reaction. High-purity powders of $Ba(NO_3)_2$ (Rare Metallic, Japan, 99.99 %), SnO_2 (Kojundo Chemical Laboratory, Japan, 99.99 %), and Ta_2O_5 (Rare Metallic, 99.99 %) were weighed in the desired proportions and milled for 1 h in an agate mortar. The mixed powder was calcined at 813 K for 1 h in flowing argon and subsequently was calcined at 853 K for 6 h in flowing argon. The calcined powder was uniaxially pressed into a pellet at 49 MPa. The green compact, which was pressed at 245 MPa using the cold isostatic pressing (CIP) method after being wrapped in platinum, was covered with a boron nitride (BN) powder and was sealed in a Pyrex glass tube under vacuum. Densification was achieved using the hot isostatic pressing (HIP) method for 4 h at 1273 K in an atmosphere of argon gas, and the maximum pressure was 196 MPa [8].

The crystal phases of the sintered samples were examined by powder X-ray diffraction (XRD, RAD-2200, Rigaku, Japan) using monochromatic CuKα radiation (Kα₁ = 1.5405 Å). The lattice parameter was determined from high-angle reflections with Si as a standard. The bulk density was measured using the Archimedes method. Scanning electron microscopy (SEM, Model JSM-7001FD, JEOL, Japan) was used for microstructural observation. The atomic percentages of Ba, Sn, and Ta were determined using energy-dispersive X-ray spectroscopy (EDS, Model JED-2300, JEOL). The binding energy of the Ta 4f level was measured using X-ray photoelectron spectroscopy (XPS, Model AXIS-165, Kratos, UK) with monochromatic MgKα radiation (1253.6 eV) at room temperature. The binding energy was calibrated against the C1 s level from residual hydrocarbon molecules. Electrical conductivity and the Seebeck coefficient were measured using the electrical conductivity & Seebeck coefficient measurement system (RZ2001i, Ozawa, Japan).
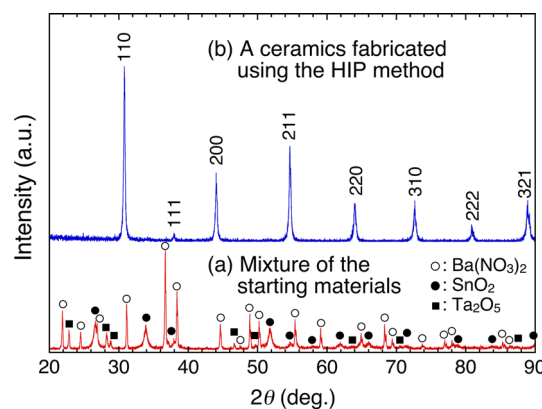

Fig. 1 XRD patterns: **a** a mixture ($x = 0.06$) of the starting materials, **b** the $Ba(Sn_{0.94}Ta_{0.06})O_3$ ($x = 0.06$) ceramics fabricated using the HIP method at 1273 K and 196 MPa for 4 h in an atmosphere of argon gas

Table 1 The lattice parameter (a), relative density (D), atomic percentage, and activation energy for hopping (E_h) of the $Ba(Sn_{1-x}Ta_x)O_3$ ceramics

x	a (Å)	D (%)	Atomic percent (%)			E_h (eV)
			Ba	Sn	Ta	
0.01	4.1204 (2)	94.4	50.0	49.4	0.6	0.02
0.03	4.1194 (2)	93.4	50.9	47.4	1.7	0.04
0.04	4.1193 (1)	92.7	49.3	48.6	2.1	0.04
0.06	4.1186 (1)	92.8	50.4	46.0	3.6	0.05

Results and discussion

According to Upadhyay et al. [9], the relative density of $BaSnO_3$ that was sintered at 1525 K in air was ca. 80 %. In the present study, therefore, the HIP method was used to obtain $Ba(Sn_{1-x}Ta_x)O_3$ ceramics with high relative densities. Figure 1 shows the XRD patterns of both a mixture ($x = 0.06$) of the starting materials and the $Ba(Sn_{0.94}Ta_{0.06})O_3$ ($x = 0.06$) ceramic fabricated using the HIP method. After HIP processing, all diffraction peaks of the XRD pattern were completely indexed as the perovskite-type structure in the range of $0.01 \leq x \leq 0.06$ [1]. The lattice parameter decreased slightly from 4.1204 Å ($x = 0.01$) to 4.1186 Å ($x = 0.06$), as shown in Table 1. The relative densities of $Ba(Sn_{1-x}Ta_x)O_3$ ceramics were high (92.7–94.4 %) regardless of x, as shown in Table 1. SEM images of the fracture surface are shown in Fig. 2. The average particle size decreased slightly from ca. 2 μm ($x = 0.01$) to ca. 1.5 μm ($x = 0.06$). The atomic percentage of Ta determined from the EDS measurement increased linearly with increasing x, as shown in Table 1. The results of the XRD and EDS measurements indicated that the Sn ions had been replaced by the Ta ions in $Ba(Sn_{1-x}Ta_x)O_3$ ceramics.
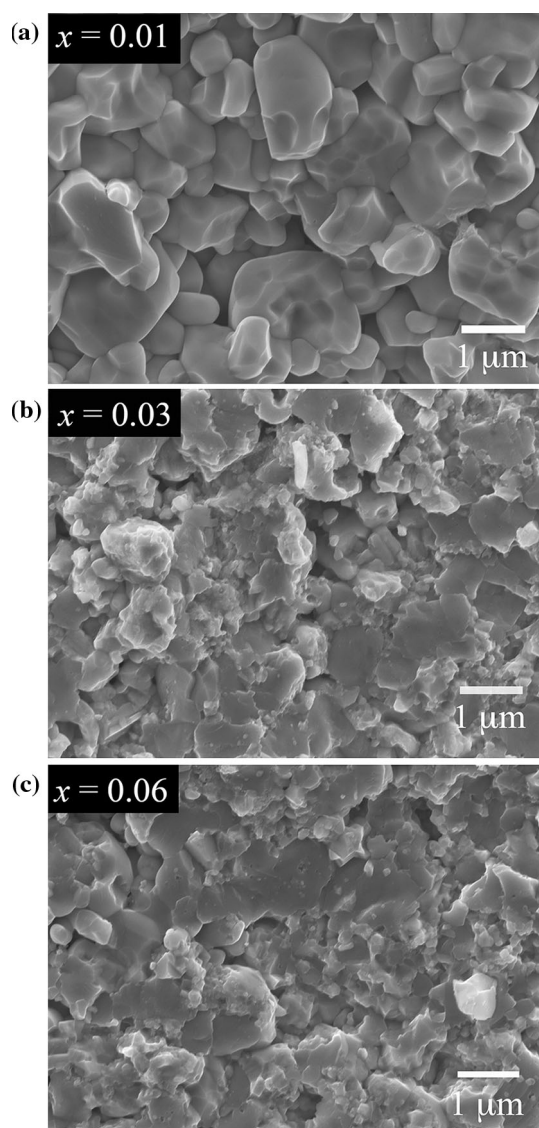
Fig. 2 SEM images of the fracture surfaces of the $Ba(Sn_{1-x}Ta_x)O_3$ ($x = 0.01$, 0.03, and 0.06) ceramics

Fig. 3 The measured Ta4f XPS spectra of the $Ba(Sn_{1-x}Ta_x)O_3$ ceramics

The measured Ta4f XPS spectra of the $Ba(Sn_{1-x}Ta_x)O_3$ ceramics are shown in Fig. 3. The peak of the Ta4f level was broad and unsymmetrical. Hashimoto et al. used an anodic oxidized Ta_2O_5 thin film on a tantalum plate for the XPS measurement [10]. The binding energies of the Ta^{5+}, Ta^{4+}, Ta^{3+}, and Ta^0 levels were 27.5–29.2, 28.6–25.6, 24.0–26.0 and 22.4–24.0 eV, respectively. Yan et al. measured the XPS spectra of $LiTaO_3$ wafers and reported that the binding energies of the Ta4f level were ca. 28.4 (Ta^{5+}) and ca. 27.1 eV (Ta^{4+}) [11]. In the present $Ba(Sn_{1-x}Ta_x)O_3$ ceramics, since the binding energy of the Ta4f level was 29.3–29.7 eV, it is thought that the Ta^{5+} ion was stable in $Ba(Sn_{1-x}Ta_x)O_3$ ceramics and that the broad peak was the overlap between the $Ta^{5+}4f_{5/2}$ and $Ta^{5+}4f_{7/2}$ levels [11]. According to Shannon [12], the ionic radii of the Sn^{4+}
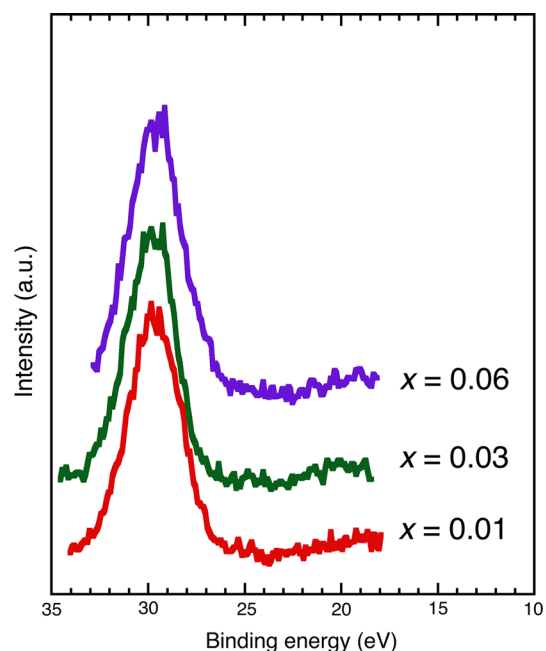
ion and the Ta^{5+} ion with a coordination of 6 are 0.69 Å and 0.64 Å, respectively. Therefore, the slight decrease in the lattice parameter as shown in Table 1 was explained by the difference in the ionic radii between the Sn^{4+} and Ta^{5+} ions.

The electrical resistivities (ρ) of the $Ba(Sn_{1-x}Ta_x)O_3$ ceramics decreased slightly with the rise of temperature (T), and the log ρ–$1000/T$ curve deviated from a straight line at high temperature, as shown in Fig. 4. Omeiri et al. reported that the electrical resistivity of $BaSnO_3$ was very high and was assumed to be more than 10^8 Ω cm [13]. However, the electrical resistivities of the present $Ba(Sn_{1-x}Ta_x)O_3$ ceramics were extremely low at $x = 0.01$ and increased with increasing x in the range of $0.01 \le x \le 0.06$. Since the variation in the relative densities of $Ba(Sn_{1-x}Ta_x)O_3$ ceramics was 2 % or less, it is thought that relative density hardly affected the electrical resistivity. According to Singh et al. [7], the electrical resistivity of $Ba(Sn_{1-x}Nb_x)O_3$ decreased with increasing x in the range of $0.001 \le x \le 0.01$ and then increased with increasing x in the range of $0.01 \le x \le 0.10$. The decrease in the electrical resistivity up to $x = 0.01$ was explained by an increase in the number of electrons released from both the Nb ion on the Sn lattice site and an oxygen vacancy. On the other hand, the increase in the electrical resistivity for $x > 0.01$ was explained by an increase in impurity scattering due to the presence of Nb^{5+} ions. In the present $Ba(Sn_{1-x}Ta_x)O_3$ ceramics, XPS and EDS measurements indicated that the valence of the Ta ion was 5+ and that the atomic percentage of Ta increased with increasing
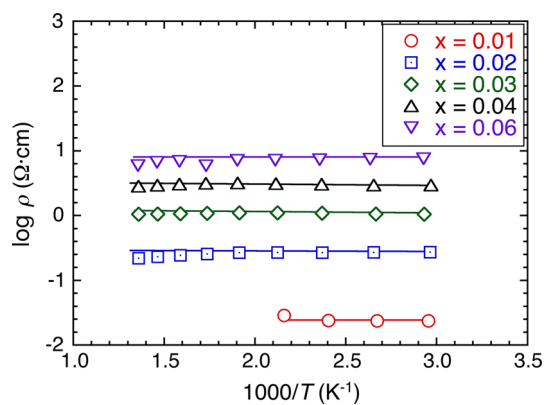
Fig. 4 The relationship between log ρ of the $Ba(Sn_{1-x}Ta_x)O_3$ ceramics and $1000/T$

Fig. 5 The relationship between logged σT of the $Ba(Sn_{1-x}Ta_x)O_3$ ceramics and $1000/T$

x. Therefore, it is thought that the electrical resistivities of the $Ba(Sn_{1-x}Ta_x)O_3$ ceramics increased as a result of impurity scattering due to the presence of Ta^{5+} ions in the same manner as $Ba(Sn_{1-x}Nb_x)O_3$ [7].

Singh et al. reported that the released electrons in $Ba(Sn_{1-x}Nb_x)O_3$ were captured by the Nb^{5+} ions or the Sn^{4+} ions, and that the Nb^{4+} ions or the Sn^{3+} ions were generated [7]. Accordingly, electrical conduction occurred by the hopping of electrons between the Nb^{5+} and Nb^{4+} ions or between the Sn^{4+} and Sn^{3+} ions. Electrical conductivity (σ) for hopping in a small polaron model is given by.

$$\sigma = \frac{A}{T}\exp\left(-\frac{E_h}{k_B T}\right),$$

where A is a constant, E_h is the activation energy for hopping, and k_B is the Boltzmann constant [14]. Since the log σT–$1000/T$ curves of the $Ba(Sn_{1-x}Ta_x)O_3$ ceramics were linear in the measured temperature range as shown in Fig. 5, it is thought that $Ba(Sn_{1-x}Ta_x)O_3$ ceramics exhibited electrical conductivity for hopping in the small polaron model. We could not obtain data on electrical resistivity or the Seebeck coefficient above 463 K because the ceramics ($x = 0.01$) broke during the measurement. According to Taguchi [15], the electrical resistivity of K_2NiF_4-type $Ca_2(Mn_{1-x}Nb_x)O_4$ decreased extremely in the range of $0 \leq x \leq 0.05$ because electron transfer on the Mn^{3+}–O–Mn^{4+} path became active as the Mn^{3+} ion increased. In the range of $0.05 \leq x \leq 0.15$, however, the decrease in electrical resistivity was very slight because the Nb^{5+} ion, which had no $4d$ electron, prevented electron transfer on the Mn^{3+}–O–Mn^{4+} path. In the present $Ba(Sn_{1-x}Ta_x)O_3$ ceramics, it is predicted that the Ta^{5+} ion, which had no $5d$ electron, prevented electron transfer on the Sn–O–Sn path. The activation energy for hopping (E_h) increased slightly from 0.02 ($x = 0.01$) to 0.05 eV ($x = 0.06$), as shown in Table 1. This result indicates that impurity
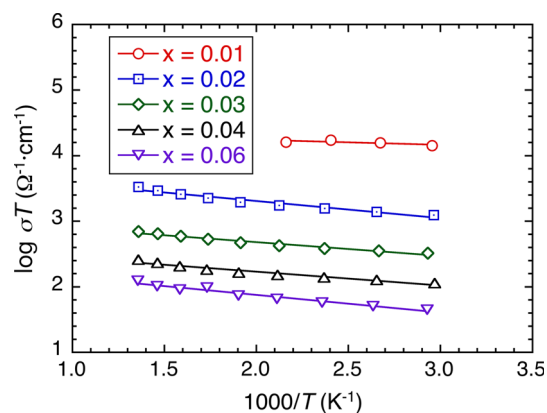
scattering due to the presence of the Ta ions was more dominant than conduction via hopping in the $Ba(Sn_{1-x}Ta_x)O_3$ ceramics.

The temperature dependence of the Seebeck coefficient (S) of the $Ba(Sn_{1-x}Ta_x)O_3$ ceramics is shown in Fig. 6. Since the Seebeck coefficient was negative, $Ba(Sn_{1-x}Ta_x)O_3$ ceramics were n-type semiconductors and the carrier was an electron. The absolute value of the Seebeck coefficient increased with increasing temperature and x. The temperature dependence of the power factor ($S^2\sigma$) of the $Ba(Sn_{1-x}Ta_x)O_3$ ceramics is shown in Fig. 7. The power factor increased with the rise in temperature and decreased with increasing x despite the slight increase in the absolute value of the Seebeck coefficient. The $Ba(Sn_{0.99}Ta_{0.01})O_3$ ceramics had electrical conductivity with 35–42 Ω^{-1} cm^{-1} and the absolute value of the Seebeck coefficient was 43–53 μV/K. Therefore, the $Ba(Sn_{0.99}Ta_{0.01})O_3$ ceramics had a maximum power factor (ca. 1.0×10^{-5} W m^{-1} K^{-2}) at 463 K. Yasukawa et al. reported the thermal properties of the $Ba(Sn_{1-x}Co_x)O_3$ ceramics prepared at 1673 K in air using a solid-state reaction [6]. Electrical conductivity and the Seebeck coefficient at 470 K were 0.016–0.06 Ω^{-1} cm^{-1} and 30–45 μV/K, respectively. Although there was almost no difference in the absolute value of the Seebeck coefficient between the $Ba(Sn_{1-x}Co_x)O_3$ ceramics and the $Ba(Sn_{1-x}Ta_x)O_3$ ceramics, the $Ba(Sn_{1-x}Co_x)O_3$ ceramics had lower electrical conductivity by two to three orders of magnitude compared with the $Ba(Sn_{1-x}Ta_x)O_3$ ceramics. Therefore, the power factor of the $Ba(Sn_{0.85}Co_{0.15})O_3$ ceramics was very low (ca. 6.0×10^{-9} W m^{-1} K^{-2} at 470 K). The $(Ba_{0.95}La_{0.05})SnO_3$ ceramics were synthesized using a polymerized complex method [16]. Electrical conductivity was 0.2–0.4 Ω^{-1} cm^{-1} at 400–700 K. The absolute value of the Seebeck coefficient was 40–60 μV/K at 400–700 K; this was almost equal to that of the $Ba(Sn_{1-x}Ta_x)O_3$ ceramics. The power factor was ca. 1.0×10^{-7}

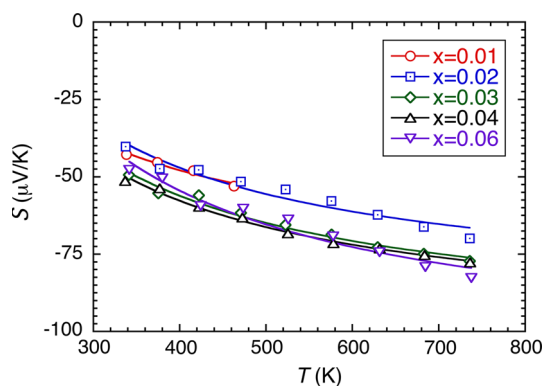**Fig. 6** The temperature dependence of the Seebeck coefficient (S) of the $Ba(Sn_{1-x}Ta_x)O_3$ ceramics

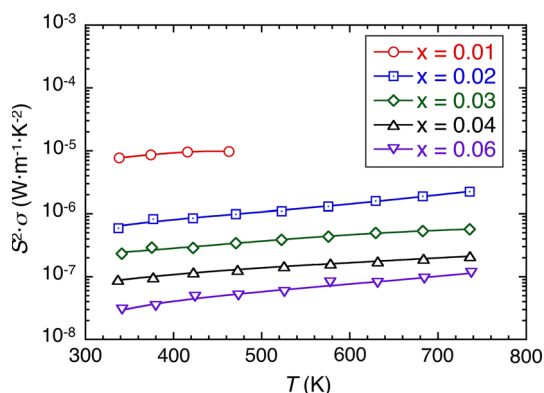**Fig. 7** The temperature dependence of the power factor ($S^2\sigma$) of the $Ba(Sn_{1-x}Ta_x)O_3$ ceramics

W m^{-1} K^{-2} at 400–700 K. Subsequently, Yasukawa et al. fabricated $(Ba_{1-x}La_x)SnO_3$ ceramics with relative densities of 93–97 % using the subsequent spark plasma sintering (SPS) technique [3]. The absolute value of the Seebeck coefficient and electrical conductivity at 400–700 K were 40–65 µV/K and 400–500 Ω^{-1} cm^{-1}, respectively. Although there was no difference in the Seebeck coefficients between the $(Ba_{1-x}La_x)SnO_3$ ceramics fabricated using the polymerized complex method and those fabricated using the SPS method, the latter had greater electrical conductivity. As a result, the power factor of the $(Ba_{0.99}La_{0.01})SnO_3$ ceramics using the SPS method was high (ca. 2.8×10^{-4} W m^{-1} K^{-2}) at 1073 K. These results indicate that the improvement of the electrical conductivity of the $BaSnO_3$ ceramics is very important to obtain a high power factor.

Conclusions

The perovskite-type $Ba(Sn_{1-x}Ta_x)O_3$ ceramics were fabricated in the range of $0.01 \leq x \leq 0.06$ using the HIP method at 1273 K and 196 MPa for 4 h in an atmosphere of argon gas. The relative densities were 92.7–95.1 % regardless of x. The lattice parameter decreased slightly from 4.1204 Å ($x = 0.01$) to 4.1186 Å ($x = 0.06$), and the atomic percentage of Ta increased linearly with increasing x. The electrical resistivity increased with increasing x, indicating that impurity scattering due to the presence of Ta^{5+} ions was more dominant than conduction via hopping between the Ta^{5+} and Ta^{4+} ions or between the Sn^{4+} and Sn^{3+} ions. $Ba(Sn_{1-x}Ta_x)O_3$ ceramics were n-type semiconductors, and the absolute value of the Seebeck coefficient increased with increasing temperature and x. The power factor was high (ca. 1.0×10^{-5} W m^{-1} K^{-2}) at $x = 0.1$ because the decrease in σ exceeded the slight increase in S^2.

References

1. Maekawa T, Kurosaki K, Yamanaka S (2006) Thermal and mechanical properties of polycrystalline BaSnO$_3$. J Alloys Compd 416:214–217
2. Smith MG, Goodenough JB, Manthiram A, Taylor RD, Penf W, Kimball W (1992) Tin and antimony valence state in BaSn$_{0.86}$Sb$_{0.15}$O$_{3-\delta}$. J Solid State Chem 98:181–186
3. Yasukawa M, Kono T, Ueda K, Yanagi H, Hosono H (2010) High-temperature thermoelectric properties of La-doped BaSnO$_3$ ceramics. Mater Sci Eng B 173:29–32
4. Upadhyay S, Dahu AK, Kumar D, Parkash O (1998) Probing electrical conduction behavior of BaSnO$_3$. J Appl Phys 84:828–832
5. Trari M, Doumerc JP, Dordor P, Pouchard M, Behr G, Krabbes G (1994) Preparation and characterization of lanthanum doped BaSnO$_3$. J Phys Chem Solids 55:1239–1243
6. Yasukawa M, Hamada Y, Kono T, Ueda K, Yanagi H, Kim SW, Hosono H (2011) Thermoelectric properties of p-type BaSnO$_3$ ceramics doped with cobalt. J Jpn Soc Powder Powder Metall 58:149–154
7. Singh P, Parkash O, Kumar D (2005) Electrical conduction behavior of perovskite oxide system BaSn$_{1-x}$Nb$_x$O$_3$. Solid State Ion 176:2167–2170
8. Hirota K, Takano Y, Yoshinaka M, Yamaguchi O (2001) Hot isostatic pressing of chromium nitrides (Cr$_2$N and CrN) prepared by self-propagating high-temperature synthesis. J Am Ceram Soc 84:2120–2122
9. Upadhyay S, Parkash O, Kumar D (1997) Preparation and characterization of barium stannate BaSnO$_3$. J Mater Sci Lett 16:1330–1332
10. Hashimoto S, Tanaka C, Murata A, Sakurada T (2006) Formulation for XPS spectral change of oxides by Ar ion bombardment: application of the formulation to Ta$_2$O$_5$ system. J Surf Anal 13:14–16
11. Yan T, Zheng F, Yu Y, Qin S, Liu H, Wang J, Yu D (2011) Formation mechanism of black LiTaO$_3$ single crystals through chemical reduction. J Appl Cryst 44:158–162

12. Shannon RD (1976) Revised effective ionic radii and systematic studies of interatomic distances in halides and chalcogenides. Acta Cryst A 32:751–767

13. Omeiri S, Hadjarab B, Bouguelia A, Trari M (2010) Electrical, optical and photoelectrochemical properties of $BaSnO_{3-\delta}$. J Alloys Compd 505:592–597

14. Böttger H, Bryksin VV (1976) Hopping conductivity in ordered and disordered solids. Phys Status Solidi (b) 78:9–56

15. Taguchi H (2001) Electrical property of K_2NiF_4-type $Ca_2(Mn_{1-x}Nb_x)O_4$. Mater Res Bull 36:1361–1367

16. Yasukawa M, Ikeuchi K, Kono T, Yanagi H, Hosono H (2007) Preparation of semiconductive La-doped $BaSnO_3$ by a polymerized complex method and the thermoelectrical properties. J Jpn Soc Powder Powder Metall 54:639–644